Mechanistic Investigations of an Enantioselective Hydrogenation Catalyzed by a Ruthenium−BINAP Complex. 1. Stoichiometric and Catalytic Labeling Studies

Jason A. Wiles and Steven H. Bergens*

Department of Chemistry, University of Alberta, Edmonton, Alberta T6G 2G2

Received February 19, 1998

The enantioselective hydrogenation of (*Z*)-methyl α-acetamidocinnamate ((*Z*)-MAC) is catalyzed by [Ru((*R*)-BINAP)(H)(MeCN)$_n$(sol)$_{3-n}$](BF$_4$) (**2**, $n = 0-3$, sol = acetone or methanol, (*R*)-BINAP = (*R*)-2,2′-bis(diphenylphosphino)-1,1′-binaphthyl) in up to 94% ee (*R*). The mechanism of this catalytic hydrogenation was investigated using in situ NMR spectroscopy, and by comparing the stereochemistry and regiochemistry of deuterium-labeling studies carried out on the catalytic reaction to those carried out on an isolated, possible catalytic intermediate. The isolated species is the olefin−hydride insertion product, [Ru((*R*)-BINAP)-((*S*)-MACH)(MeCN)](BF$_4$) ((S_{C_α})-**1**). Compound (S_{C_α})-**1** is the only species present in detectable amounts, by ^{1}H and ^{31}P NMR spectroscopy, during the catalytic hydrogenation at room temperature. The absolute configuration at the stereogenic α-carbon of MACH is the same (assuming stereospecific replacement of ruthenium with hydrogen) as that of the major enantiomer of the catalytic hydrogenation ((*R*)-*N*-acetylphenylalanine methyl ester ((*R*)-MACH$_2$)). Results obtained from the stoichiometric hydrogenolysis and deuteriolysis of (S_{C_α})-**1**, from the catalytic deuteration of (*E*)-MAC and (*Z*)-MAC, and from the reaction of (S_{C_α})-**1** with excess (*Z*)-MAC-Me-d_3 all indicate that formation of (S_{C_α})-**1** is rapid and reversible prior to the irreversible hydrogenolysis of the ruthenium−carbon bond. The sum of the stereoselectivities and regioselectivities of the formation and hydrogenolysis of (S_{C_α})-**1** equals the stereoselectivity and regioselectivity of the catalytic hydrogenation. Solvolysis of the ruthenium−carbon bond occurs to less than 4% during the catalytic hydrogenation carried out in methanol. Removal of MeCN from the catalyst system has no effect on the enantioselection of the catalytic hydrogenation.

Introduction

We report and compare results obtained from deuterium-labeling studies on a putative catalytic intermediate to those obtained from the overall catalytic cycle for the enantioselective hydrogenation of (*Z*)-methyl α-acetamidocinnamate ((*Z*)-MAC) using a ruthenium−((*R*)-BINAP) system as catalyst ((*R*)-BINAP = (*R*)-2,2′-bis(diphenylphosphino)-1,1′-binaphthyl). Complexes of ruthenium(II) and BINAP are among the most successful catalyst systems for the enantioselective hydrogenation of prochiral olefins and ketones.[1] Despite the high enantiomeric excesses (ee's) and turnover numbers that often distinguish these systems, the asymmetric interactions that are responsible for their enantioselection are unknown.[2,3] Among the reasons that enantioselective interactions have not been elucidated for these hydrogenations is that all reported observations of putative catalytic intermediates are either incomplete,[4] providing little information about how the substrate is bonded to ruthenium, or they are of species in which the substrate is not bonded to ruthenium through a prochiral functionality.[5] In a recent communication,[6] we reported

* To whom correspondence should be addressed. E-mail: Steve.Bergens@ualberta.ca.

(1) (a) Ager, D. J.; Laneman, S. A. *Tetrahedron: Asymmetry* **1997**, *8*, 3327−3355. (b) Noyori, R. *Acta Chem. Scand.* **1996**, *50*, 380−390. (c) Kumobayashi, H. *Recl. Trav. Chim. Pays-Bas* **1996**, *115*, 201−210. (d) Akutagawa, S. *Appl. Catal., A* **1995**, *128*, 171−207. (e) Noyori, R. *Asymmetric Catalysis in Organic Synthesis*; Wiley: New York, 1994. (f) Noyori, R. *Tetrahedron* **1994**, *50*, 4259−4292. (g) Takaya, H.; Ohta, T.; Noyori, R. In *Catalytic Asymmetric Synthesis*; Ojima, I., Ed.; VCH: New York, 1993; Chapter 1. (h) Noyori, R. *CHEMTECH* **1992**, *22*, 360−367. (i) Noyori, R. *Science* **1990**, *248*, 1194−1199. (j) Noyori, R.; Takaya, H. *Acc. Chem. Res.* **1990**, *23*, 345−350. (k) Noyori, R.; Kitamura, M. In *Modern Synthetic Methods 1989*; Scheffold, R., Ed.; Springer-Verlag: Berlin, 1989; pp 115−198. See also ref 6 and references therein.

(2) For representative examples of mechanistic investigations of hydrogenations catalyzed by ruthenium−BINAP complexes, see: (a) Chan, A. S. C.; Chen, C. C.; Yang, T. K.; Huang, J. H.; Lin, Y. C. *Inorg. Chim. Acta* **1995**, *234*, 95−100. (b) Brown, J. M.; Rose, M.; Knight, F. I.; Wienand, A. *Recl. Trav. Chim. Pays-Bas* **1995**, *114*, 242−251. (c) Brown, J. M. *Chem. Soc. Rev.* **1993**, 25−41. (d) Kawano, H.; Ikariya, T.; Ishii, Y.; Saburi, M.; Yoshikawa, S.; Uchida, Y.; Kumobayashi, H. *J. Chem. Soc., Perkin Trans. 1* **1989**, 1571−1575.

(3) The mechanism of the enantioselective hydrogenation of (*Z*)-MAC catalyzed by rhodium−bis(phosphine) complexes is well documented: (a) Giovannetti, J. S.; Kelly, C. M.; Landis, C. R. *J. Am. Chem. Soc.* **1993**, *115*, 4040−4057. (b) Landis, C. R.; Halpern, J. *J. Am. Chem. Soc.* **1987**, *109*, 1746−1754. (c) Brown, J. M.; Chaloner, P. A.; Morris, G. A. *J. Chem. Soc., Perkin Trans. 2* **1987**, 1583−1588. (d) Halpern, J. *Science* **1982**, *217*, 401−407. (e) Brown, J. M.; Chaloner, P. A. *J. Am. Chem. Soc.* **1980**, *102*, 3040−3048. For enantioselective reductions of α-aminoacrylic acid derivatives by dideuterium gas catalyzed by rhodium−bis(phosphine) complexes, see: (f) Burk, M. J.; Feaster, J. E.; Nugent, W. A.; Harlow, R. L. *J. Am. Chem. Soc.* **1993**, *115*, 10125−10138. (g) Scott, J. W.; Keith, D. D.; Nix, G., Jr.; Parrish, D. R.; Remington, S.; Roth, G. P.; Townsend, J. M.; Valentine, D., Jr.; Yang, R. *J. Org. Chem.* **1981**, *46*, 5086−5093. (h) Detellier, C.; Gelbard, G.; Kagan, H. B. *J. Am. Chem. Soc.* **1978**, *100*, 7556−7561. (i) Koenig, K. E.; Knowles, W. S. *J. Am. Chem. Soc.* **1978**, *100*, 7561−7564.

S0276-7333(98)00113-7 CCC: $15.00
Publication on Web 04/28/1998

the first observation and structural characterization of a ruthenium−BINAP complex with a substrate bonded to ruthenium through a stereogenic carbon center derived from the prochiral functionality of the substrate. The complex [Ru((*R*)-BINAP)((*S*)-MACH)(MeCN)](BF_4) ((S_{C_α})-**1**) results from the stoichiometric or catalytic (excess substrate) reaction between (*Z*)-MAC and the catalyst system [Ru((*R*)-BINAP)(H)(MeCN)$_n$(sol)$_{3-n}$](BF_4) (**2**, $n = 0-3$, sol = acetone or methanol)[7] at room temperature. Compound (S_{C_α})-**1** is the product of olefin−hydride insertion with placement of ruthenium at the α-olefin carbon of (*Z*)-MAC (eq 1). To identify with

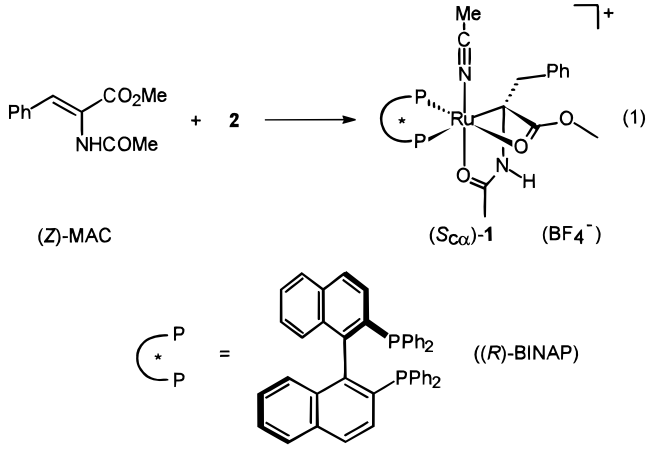

reasonable certainty that (S_{C_α})-**1** or any species observed during an enantioselective catalytic reaction is a catalytic intermediate leading to the major enantiomer of the product, the following criteria must be satisfied: (1) the absolute configuration of the putative intermediate must directly extrapolate to that of the major enantiomer of the product. Although satisfaction of this criterion does not constitute proof of the authenticity of the putative interemediate, failure to satisfy this criterion is proof that the species is not an intermediate leading to the major enantiomer. (2) The stereoselectivities and regioselectivities (as determined by isotopic labeling or other probes) of the stoichiometric reactions forming the putative intermediate and of the reactions converting it to product (and free catalyst) must summate to give the overall stereoselectivity and regioselectivity of the catalytic reaction. (3) The kinetics of the stoichiometric reactions forming the putative intermediate and those of the reactions converting it to product (and free catalyst) must comprise at least a component of the overall kinetics of the catalytic cycle. In addition to this information, the identities and kinetics of the enantioselective step(s) must be obtained to determine if the asymmetric interactions in the putative intermediate are relevant to the origins of enantioselection by the catalytic reaction. As part of our efforts to determine if (S_{C_α})-**1** is an authentic catalytic intermediate, we report the stereoselectivity and regioselectivity of the olefin−hydride insertion forming (S_{C_α})-**1**, the stereoselectivity and regioselectivity of the reverse *β*-hydride elimination, and the extent to which formation of (S_{C_α})-**1** is reversible prior to hydrogenolysis of the ruthenium−carbon bond. These results will be compared to the stereoselectivity and regioselectivity of the catalytic hydrogenation. We also report the extent of solvolysis of the ruthenium−carbon bond during catalytic hydrogenations carried out in methanol solution and the effect of removing MeCN from the system on the catalytic enantioselectivity.

Table 1. Hydrogenation of (*Z*)-MAC Catalyzed by 2[a]

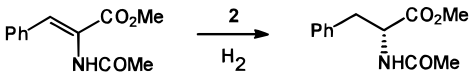

entry	$P(H_2)$, atm	solvent	*T*, °C	ee, % (*R*)
1	2	acetone	30	94
2	4	acetone	30	92
3	20	acetone	30	83
4	50	acetone	30	75
5	4	acetone	50	92
6	4	acetone	10	93
7	4	MeOH	30	87
8	4	THF	30	85
9	4	CH_2Cl_2	30	64
10	50	MeCN	30	no reaction

[a] Reaction conditions: 2 mol % **2**; [**2**] = 2.6 mM; stir rate = 1100 rpm; 100% conversion except where noted otherwise.

Results and Discussion

Optimization of the Catalytic Hydrogenation. The pressure of dihydrogen gas, the solvent, and temperature were varied to optimize the hydrogenation of (*Z*)-MAC using **2** as the catalyst. Table 1 summarizes our results. Among the solvents surveyed, the highest enantiomeric excess (ee) was obtained in acetone, being even higher than that in methanol, a common solvent for hydrogenations using ruthenium−BINAP catalyst systems.[1] The turnover frequency[8] was higher in acetone (∼0.9 min^{-1}) than in methanol (∼2.7 × 10^{-2} min^{-1})[7] as well. Although we have not determined the maximum turnover number in acetone, we achieved 980 turnovers in 91% ee (*R*) after 4 days at 30 °C under 4 atm of dihydrogen gas.

The ee in acetone solution decreased as the dihydrogen pressure was increased (Table 1). Inverse relationships between ee and dihydrogen pressure have been reported for other catalyst−substrate systems.[1e] Barring mass transfer effects,[9] an inverse relationship between ee and pressure of dihydrogen gas often implies

(4) (a) King, S. A.; DiMichele, L. In *Catalysis of Organic Reactions*; Scaros, M. G., Prunier, M. L., Eds.; Marcel Dekker: New York, 1995; Vol. 62, pp 157−166. (b) Saburi, M.; Takeuchi, H.; Ogasawara, M.; Tsukahara, T.; Ishii, Y.; Ikariya, T.; Takahashi, T.; Uchida, Y. *J. Organomet. Chem.* **1992**, *428*, 155−167. (c) Ohta, T.; Takaya, H.; Noyori, R. *Tetrahedron Lett.* **1990**, *31*, 7189−7192.

(5) (a) Ashby, M. T.; Khan, M. A.; Halpern, J. *Organometallics* **1991**, *10*, 2011−2015. (b) Ashby, M. T.; Halpern, J. *J. Am. Chem. Soc.* **1991**, *113*, 589−594.

(6) Wiles, J. A.; Bergens, S. H.; Young, V. G. *J. Am. Chem. Soc.* **1997**, *119*, 2940−2941.

(7) Complex **2** is a well-defined catalyst system for a variety of transformations, including the hydrogenation of olefins. Wiles, J. A.; Lee, C. E.; McDonald, R.; Bergens, S. H. *Organometallics* **1996**, *15*, 3782−3784.

(8) These turnover frequencies were determined by setting up and taking down the pressure reactor as quickly as possible during a hydrogenation. Their values are, therefore, to be taken as approximate. Reaction conditions: 2 mol % **2**; [**2**] = 2.6 mM; stir rate = 1100 rpm; T = 30 °C; $P(H_2)$ = 4 atm.

(9) All reactions were carried out under reaction-rate-limiting conditions to eliminate gas−liquid mass transfer effects. For a study describing gas−liquid mass transfer effects on enantioselectivity, see: Sun, Y.; Landau, R. N.; Wang, J.; LeBlond, C.; Blackmond, D. G. *J. Am. Chem. Soc.* **1996**, *118*, 1348−1353.

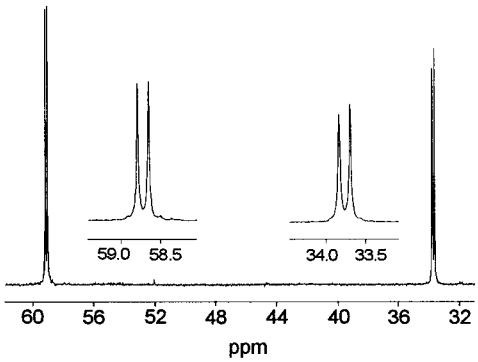

Figure 1. $^{31}P\{^1H\}$ NMR spectrum of an operating catalytic hydrogenation of (*Z*)-MAC using **2** as catalyst in acetone-d_6. The scale of the expansions is 5 times that of the original plot.

that the identity of the enantioselective step changed with the increase in dihydrogen pressure.

The ee in acetone increased slightly as the temperature was decreased from 50 to 10 °C; the turnover frequency, however, was too low to be of practical use below 10 °C. We conclude from these results that the optimum conditions for hydrogenation of (*Z*)-MAC using **2** as the catalyst are acetone solution, 30 °C, and 4 atm of dihydrogen gas.

Mechanistic Investigations. Figure 1 shows a $^{31}P\{^1H\}$ NMR spectrum recorded of an operating catalytic hydrogenation of (*Z*)-MAC after 8 turnovers under conditions (acetone, pressure of dihydrogen gas = 1 atm, 25 °C, 4 mol % **2**) similar to the optimum conditions described in the previous section.[10] Compound (S_{C_α})-**1** was the only detectable ruthenium species in solution at room temperature.[11] Similar results were obtained using methanol, tetrahydrofuran, and methylene chloride as the solvent.[12] Deuterium labeling and other experiments will show (vide infra) that it is extremely unlikely that the formation of (S_{C_α})-**1** is an irreversible kinetic trap under these conditions. Further, the catalytic hydrogenation of (*Z*)-MAC using isolated (S_{C_α})-**1** as the catalyst occurs at the same rate and ee as when **2** is used as the catalyst. Its relatively high concentration during catalysis is good evidence that (S_{C_α})-**1**, whether a catalytic intermediate or not, is the most stable ruthenium compound in solution under these conditions.

Hydrogenolysis of (S_{C_α})-1 in Acetone. The absolute configuration at the carbon center bonded to ruthenium in (S_{C_α})-**1** is *S*. Stereospecific replacement of ruthenium by hydrogen will form (*R*)-*N*-acetylphenylalanine methyl ester ((*R*)-$MACH_2$), the major enantiomer formed by the catalytic hydrogenation. As we reported in the communication, the stoichiometric reaction of (S_{C_α})-**1** with dihydrogen gas in methanol solution generated $MACH_2$ at a similar rate and ee as the catalytic hydrogenation in methanol.[6] We now report that although the stoichiometric hydrogenolysis of (S_{C_α})-**1** in acetone solution also produces $MACH_2$ in similar ee to the catalytic hydrogenation (stoichiometric, 89% (*R*) (eq 2); catalytic 92% ee (*R*)), the rate of the stoichiometric

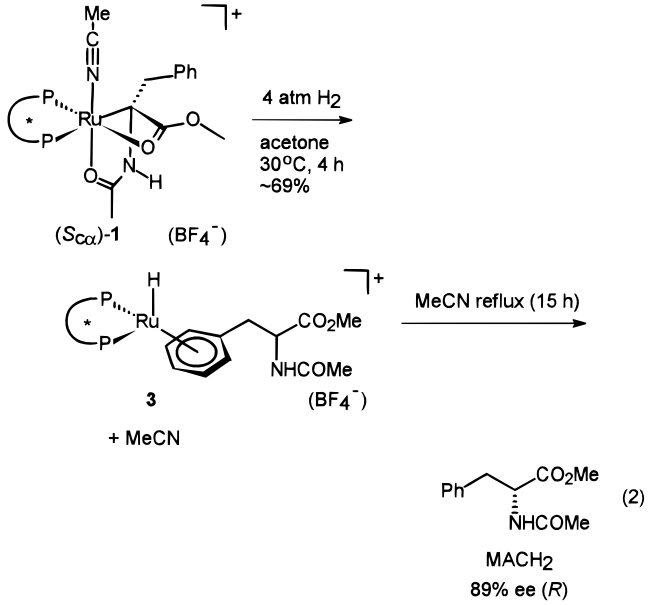

hydrogenolysis slows over the course of the reaction in this solvent. The product distribution after 4 h was 31% (S_{C_α})-**1**, 58% [Ru((*R*)-BINAP)(H)(η^6-$MACH_2$)](BF_4) (**3**, $MACH_2$ is bonded to ruthenium as an η^6-ligand through the arene ring),[6] and 11% $MACH_2$.[13] The hydrogenolysis was 97% complete after 24 h. $MACH_2$ was liberated from **3** by refluxing the mixture in MeCN solution before the ee was determined. The conditions for the stoichiometric hydrogenolysis in acetone were the same as the catalytic hydrogenation in acetone except that excess (*Z*)-MAC was absent and the concentration of (S_{C_α})-**1** was approximately 4-fold higher for the stoichiometric hydrogenolysis than for the catalytic hydrogenation. Hydrogenolysis of ruthenium−carbon bonds in coordinatively saturated 18-electron ruthenium(II) compounds has been shown to require prior ligand dissociation to generate a 16-electron intermediate. For example, the hydrogenolysis of the ruthenium−acyl bond in $RuCl(COC_7H_9)(CO)_2(PPh_3)_2$ requires prior dissociation of a triphenylphosphine ligand.[14] It is quite likely that the hydrogenolysis of (S_{C_α})-**1** proceeds via prior dissociation of the MeCN ligand to generate the 16-electron intermediate [Ru((*R*)-BINAP)((*S*)-MACH)](BF_4), which may contain a weakly coordinating acetone ligand. Since MeCN binds strongly to ruthenium(II) complexes such as (S_{C_α})-**1**,[15] the decrease in rate as the hydro-

(10) The differences between the conditions under which the spectrum was recorded and the optimum conditions for the catalytic hydrogenation resulted from the technical difficulties in carrying out such a reaction in our NMR tubes.

(11) A small amount (~8%) of one other species was detected in the ^{31}P NMR spectrum of the catalytic mixture recorded after cooling to −40 °C ($^{31}P\{^1H\}$ ($(CD_3)_2CO$, 161.9 MHz) δ 39.4 (d, $^2J_{P-P}$ = 23.6 Hz, 1P), 55.4 (d, $^2J_{P-P}$ = 23.6 Hz, 1P). This species is present in similar amounts in the ^{31}P NMR spectrum recorded at −40 °C of isolated and purified (S_{C_α})-**1**. We suspect it is either the species obtained from dissociation of acetonitrile from (S_{C_α})-**1** or it is the opposite diastereomer in equilibrium with (S_{C_α})-**1**. We have been unable to assign other signals to this species.

(12) Compound (S_{C_α})-**1** typically comprised 80−90% of the ruthenium-containing species in these solvents under these conditions. The other compounds present were mainly a mixture of [Ru((*R*)-BINAP)(H)(η^6-$MACH_2$)](BF_4) and a species which we tentatively propose as [Ru((*R*)-BINAP)(H)(η^6-(*Z*)-MAC)](BF_4). In these complexes, $MACH_2$ and (*Z*)-MAC are bound to ruthenium as η^6-arene ligands.

(13) These values were determined by ^1H NMR spectroscopy. Analysis of this mixture by ^{31}P NMR spectroscopy confirmed the presence of (S_{C_α})-**1** (35%), **3** (65%), and a number of unidentified species (quantities too low to accurately integrate). We believe that these unidentified species are decomposition products of **3** that generate uncoordinated $MACH_2$.

(14) Joshi, A. M.; James, B. R. *Organometallics* **1990**, *9*, 199−205.

Scheme 1 [a]

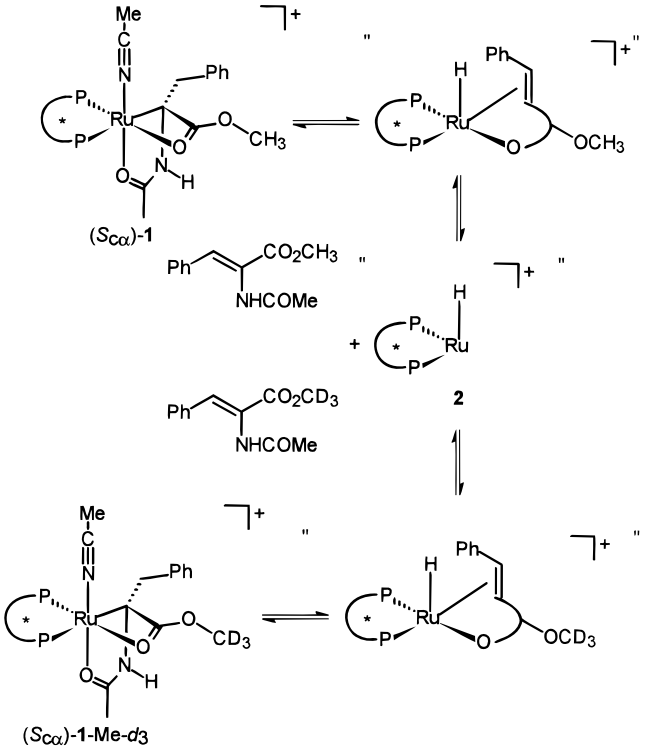

[a] Species shown in quotation marks are approximate representations of the true species in solution.

genolysis proceeded in acetone solution most likely arose from the increase in the concentration of MeCN which occurred as compound **3** accumulated in solution (eq 2). Kinetic investigations of the stoichiometric hydrogenolysis and of the catalytic hydrogenation of (*Z*)-MAC are underway, and their results will be compared in due course. We note presently that although added MeCN is a strong inhibitor of the catalytic hydrogenation of (*Z*)-MAC using **2** as the catalyst, free MeCN does not build up to detectable levels during the catalytic reaction because the excess (*Z*)-MAC in solution reacts with **2** to generate (S_{C_α})-**1**, thereby preventing formation of **3** (see Figure 1). We note further that the dissociation of MeCN prior to the hydrogenolysis of (S_{C_α})-**1** or of a related species does not contribute to the enantioselection of the catalytic reaction; the ee for the catalytic hydrogenation of (*Z*)-MAC using [Ru((*R*)-BINAP)(H)(η^6-(*rac*)-$MACH_2$)](BF_4) as the catalyst in methanol was 86% (*R*) (eq 3), in accord with that obtained using (S_{C_α})-**1** or **2** as catalysts (each giving 87% ee (*R*)).

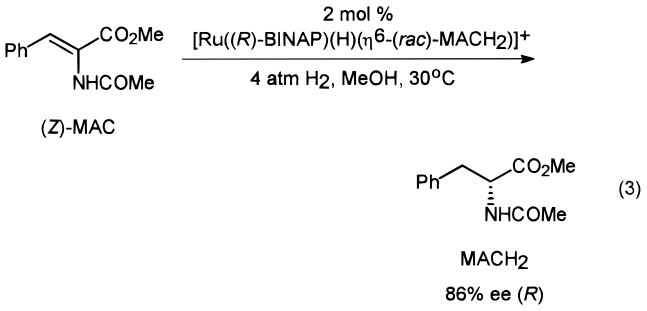

(3)

(15) No dissociation of MeCN from (S_{C_α})-**1** was observed at room temperature.

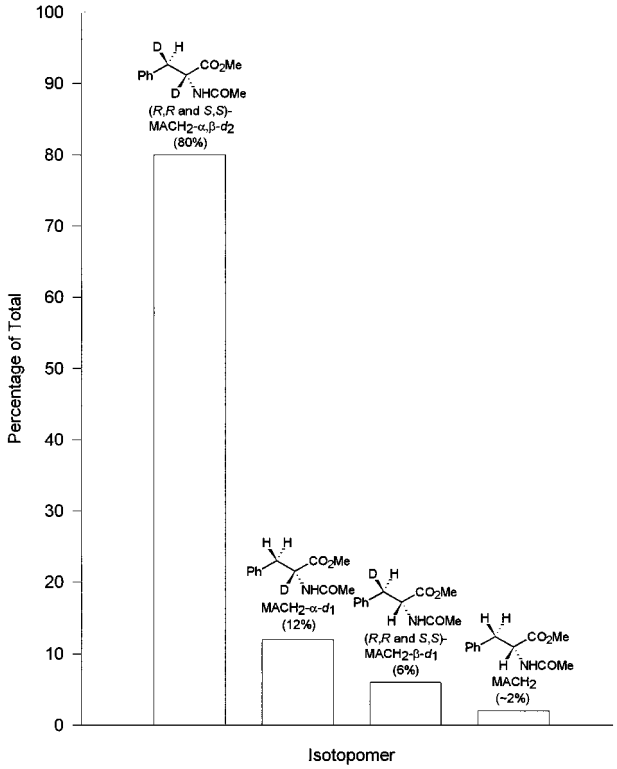

Figure 2. The distribution of $MACH_2$-d_n isotopomers from the deuteriolysis of (S_{C_α})-**1** in acetone.

Reversibility of Formation of (S_{C_α})-1. Reaction of diastereomerically pure (S_{C_α})-**1** with dihydrogen gas generated (*R*)-$MACH_2$ in ee's similar to those of the catalytic reactions in methanol and in acetone. The similar ee's for the catalytic and stoichiometric reactions indicate that formation of (S_{C_α})-**1** was to some extent reversible and that the other diastereomer(s) of (S_{C_α})-**1** reacted to form (*S*)-$MACH_2$. To confirm that its formation is reversible, compound (S_{C_α})-**1** was reacted with 2.8 equiv of (*Z*)-MAC-Me-d_3 in acetone solution at 35 °C (eq 4). The system achieved equilibrium (assuming

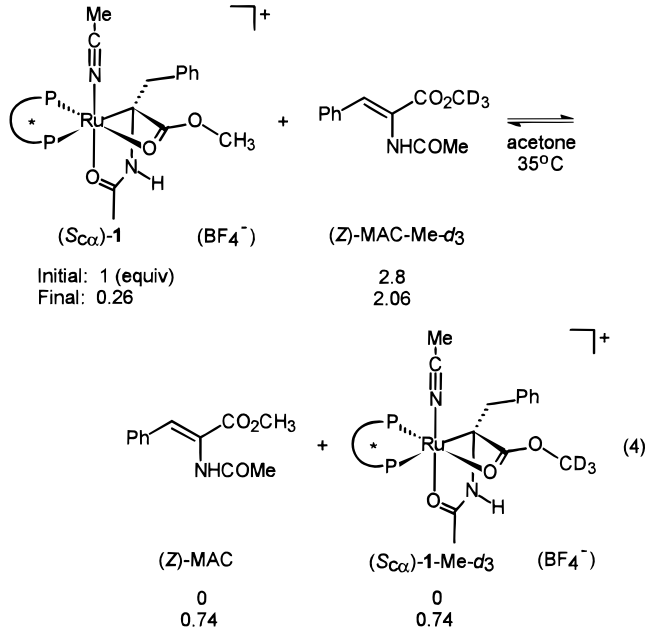

(4)

$K_{eq} = 1$), demonstrating that formation of (S_{C_α})-**1** was

reversible. Compounds (S_{C_α})-**1** and (S_{C_α})-**1**-Me-d_3 were the only ruthenium species detected in solution. Scheme 1 shows our proposed sequence of steps for the reversible formation of (S_{C_α})-**1** and (S_{C_α})-**1**-Me-d_3 from **2** reacting with (*Z*)-MAC or with (*Z*)-MAC-Me-d_3, respectively, assuming the reverse of formation of (S_{C_α})-**1** proceeds via a β-hydride elimination. β-Hydride elimination within (S_{C_α})-**1** followed by dissociation of (*Z*)-MAC would generate **2**, which can either react with (*Z*)-MAC or with (*Z*)-MAC-Me-d_3 to generate the corresponding isotopomers of (S_{C_α})-**1**. A consequence of the formation of (S_{C_α})-**1** being to some extent reversible via a β-hydride elimination on the time scale of the hydrogenolysis is that stoichiometric deuteriolysis of (S_{C_α})-**1** must form some $MACH_2$ with deuterium at the β-position. This condition on the proposed mechanism of the reverse process is investigated in the next section.

Deuterium Studies in Acetone. The stoichiometric deuteriolysis of (S_{C_α})-**1** carried out in acetone solution slowed after ~76% conversion (eq 5). Figure 2 shows

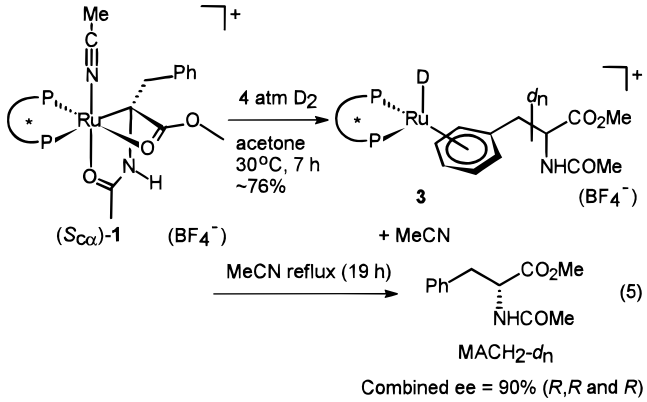

the composition of the reduced MAC after the deuteriolysis had slowed ((*R*,*R* and *S*,*S*)-$MACH_2$-α,β-d_2,[16,17] 80%; $MACH_2$-α-d_1, 12%; (*R*,*R* and *S*,*S*)-$MACH_2$-β-d_1, 6%; and $MACH_2$, ~2%). The combined ee was 90% (*R*,*R* and *R*), which is similar to that of the catalytic hydrogenation of (*Z*)-MAC in acetone (92% (*R*)). $MACH_2$ labeled by deuterium at the β-position formed as predicted by the β-hydride elimination mechanism for the reverse of formation of (S_{C_α})-**1** (Scheme 1). It is necessary to determine the reactivity of **2** toward dideuterium gas to more fully interpret these results.

Further reaction between **2** and dihydrogen gas (1 atm) was not detected by NMR spectroscopy in acetone solution over temperatures ranging from −80 to 25 °C. Reaction with dideuterium gas (1 atm), however, resulted in the immediate formation of **2**-*d*, even at temperatures well below 0 °C (eq 6).[18] Under dihydrogen gas, compound **2** is, therefore, in rapid equilibrium with small concentrations of the ruthenium(IV) trihydride [Ru((*R*)-BINAP)$(H)_3$$(MeCN)_x$$(acetone)_y$]$(BF_4)$ (**4**) (or the corresponding ruthenium(II) hydride-η^2-dihydrogen species), resulting in the observed H−D exchange with dideuterium gas. An equilibrium between **2** and **4** would, in principle, favor **2** because **4** must contain at least one mutually *trans*-disposition of a phosphine and a hydride ligand, an unfavorable situation as both of these ligands have strong *trans* influences.[19] Any free **2** generated in solution during the stoichiometric deuteriolysis of **1** is likely to quickly react with dideuterium gas to generate **2**-*d*.

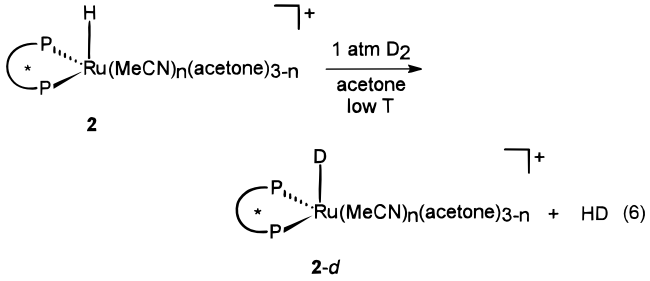

The $MACH_2$-α-d_1 (12%) produced by the stoichiometric deuteriolysis (Figure 2) almost certainly resulted from the deuteriolysis of the ruthenium−carbon bond in (S_{C_α})-**1**. The product which formed in large excess (80%) was (*R*,*R* and *S*,*S*)-$MACH_2$-α,β-d_2, with deuterium at both the α- and β-positions. This product is that of a net cis-addition of dideuterium gas to the carbon−carbon double bond of (*Z*)-MAC, and its presence is strong evidence for the formation of (S_{C_α})-1 being reversible via a β-hydride elimination. Another possibility, a stereoselective C−H activation at the β-position of $MACH_2$-α-d_1, is ruled out by our finding that reaction of $MACH_2$ with **2**-*d* under dideuterium gas does not result in H−D exchange at the α- or β-positions of $MACH_2$. Scheme 2 shows the sequence of steps involving olefin−hydride insertion and β-hydride elimination that accounts for the isotopomers of $MACH_2$-d_n produced by the stoichiometric deuteriolysis of (S_{C_α})-**1** in acetone. Elimination of the *pro*-*R*-β-hydride in (S_{C_α})-**1** followed by olefin dissociation generates (*Z*)-MAC and **2**. The stereochemistry of the β-hydride elimination will be discussed in more detail below where it will be shown that elimination of the *pro*-*S*-β-hydride within (S_{C_α})-**1** is highly unlikely. Compound **2**, generated via the β-hydride elimination, will quickly react with the excess dideuterium gas in the reactor to produce **2**-*d* (eq 6). Coordination of (*Z*)-MAC to **2**-*d* through the *si*-olefin face followed by insertion into the ruthenium−deuteride bond will generate (S_{C_α},R_{C_β})-β-d_1-**1** (of *R* absolute configuration at the deuterated β-carbon center). In strong support of this sequence of steps is that placement of acetone solutions of (S_{C_α})-**1** under lower pressures of

(16) All isotopic substitution patterns of $MACH_2$-d_n were assigned by comparison of their ^1H and ^2H NMR spectra to those of *N*-acetylphenylalanine. See ref 3h and the Experimental Section for details.

(17) For all reductions with dideuterium gas in acetone, a portion of the product was deuterated at nitrogen. In general, there was an approximate correlation between the extent of deuteration at nitrogen and the length of time the reaction was exposed to dideuterium gas in the presence of **2**. Only an approximate correlation could be obtained because H−D exchange was rapid upon exposure to even trace amounts of water. Control experiments in which $MACH_2$ was exposed to 2 mol % **2** under deuterium gas in acetone showed that **2** catalyzes the H−D exchange between the N−H bond of $MACH_2$ and dideuterium gas. We believe that deuteration at nitrogen is a side reaction which is not part of the mechanism of hydrogenation of (*Z*)-MAC catalyzed by **2**.

(18) An NMR tube containing a −80 °C argon-saturated acetone solution of **2** was quickly ejected from a cooled (−80 °C) NMR probe, injected with an excess of dideuterium gas through a rubber septum, shaken for ~15 s, and quickly returned to the probe. NMR spectra recorded at −80 °C indicated **2**-*d* was the only ruthenium species formed in solution, with concomitant formation of HD gas.

(19) Collman, J. P.; Hegedus, L. S.; Norton, J. R.; Finke, R. G. *Principles and Applications of Organotransition Metal Chemistry*; University Science Books: Mill Valley, CA, 1987.

Scheme 2

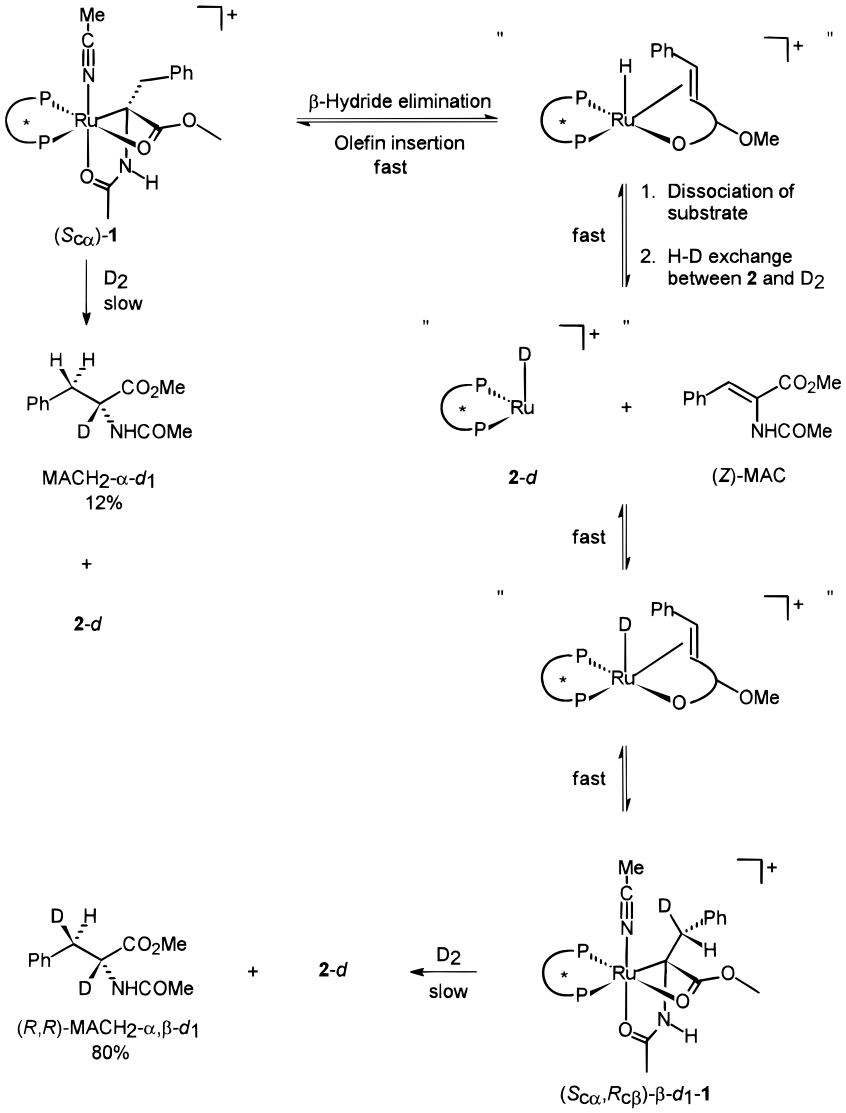

dideuterium gas (1 atm) results in H−D exchange with the *pro-R*-β-hydride. Further, reaction of **2**-*d* (made by reaction of **2** with dideuterium gas (eq 6)) with (*Z*)-MAC produced (S_{C_α},R_{C_β})-β-d_1-**1** as the only detectable ruthenium species in solution. The stereochemistry of the olefin−hydride insertion results in a net cis addition of ruthenium and hydrogen across the carbon−carbon double bond of (*Z*)-MAC. Assuming retention of configuration at the α-carbon, deuteriolysis of the ruthenium−carbon bond in (S_{C_α},R_{C_β})-β-d_1-**1** will produce (*R*,*R*)-$MACH_2$-α,β-d_2, the product of net cis addition of dideuterium to the carbon−carbon double bond of (*Z*)-MAC. (*S*,*S*)-$MACH_2$-α,β-d_2 would result from coordination of (*Z*)-MAC to **2**-*d* via the *re*-olefin face followed by deuteriolysis of the ruthenium−carbon bond.

As discussed above, β-hydride elimination and dissociation of (*Z*)-MAC from **1** during the stoichiometric deuteriolysis will produce (*Z*)-MAC and **2** in the presence of excess dideuterium gas (Scheme 2). Compound **2** in this mixture can either react with (*Z*)-MAC to regenerate (S_{C_α})-**1** (leading to $MACH_2$-α-d_1 after deuteriolysis of the ruthenium−carbon bond) or it can react with dideuterium gas to produce **2**-*d* (leading eventually to (*R*,*R* and *S*,*S*)-$MACH_2$-α,β-d_2). Since the relative rate of formation of (S_{C_α})-**1** versus that of **2**-*d* in this mixture is unknown, the 85:15 ratio of (*R*,*R* and *S*,*S*)-$MACH_2$-α,β-d_2 to $MACH_2$-α-d_1 represents the lower limit to the extent of reversibility of formation of (S_{C_α})-**1** during the deuteriolysis. We were unable to isolate $MACH_2$-α-d_1 in order to determine its ee, which would be 100% (*R*) if it formed from direct deuteriolysis of (S_{C_α})-**1** without prior formation of **2** and (*Z*)-MAC. Since the lower limit to the extent to which formation of (S_{C_α})-**1** reversed is ∼85%, equilibration between (S_{C_α})-**1**, **2**, and (*Z*)-MAC must be relatively rapid and nearly complete before deuteriolysis of the ruthenium−carbon bond occurs under these conditions.

Only the (*R*,*R*) and (*S*,*S*) diastereomers of $MACH_2$-α,β-d_2 were produced by the deuteriolysis of (S_{C_α})-**1**. This stereoselectivity is a consequence of the direct relationship between whether β-hydride or β-deuteride elimination occurred within (S_{C_α},R_{C_β})-β-d_1-**1** and the stereochemistry of the resulting MAC. This relationship also exists in the opposite diastereomer (R_{C_α},S_{C_β})-β-d_1-**1**. As shown in Scheme 3, (*Z*)-MAC will result from β-deuteride elimination and the less stable (*E*)-MAC-β-d_1 will result from β-hydride elimination. Reaction of (*E*)-MAC-β-d_1 with **2**-*d* followed by deuteriolysis of the ruthenium−carbon bond must generate $MACH_2$-α,β,β-d_3.[20] Since $MACH_2$-α,β,β-d_3 was not detected among the products,

Scheme 3

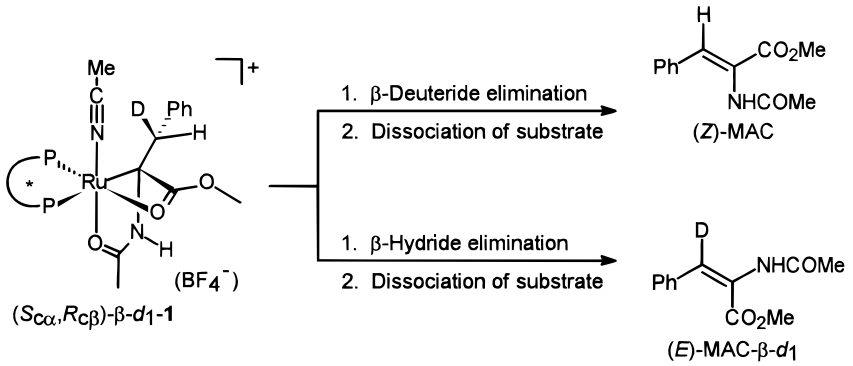

we conclude that β-hydride elimination within (S_{C_α})-**1** is highly stereoselective, favoring the *pro-R*-β-hydride in (S_{C_α})-**1** (this position is occupied by deuterium in (S_{C_α},R_{C_β})-β-d_1-**1**) and the *pro-S*-β-hydride in (R_{C_α})-**1** (this position is occupied by deuterium in (R_{C_α},S_{C_β})-β-d_1-**1**). The origins of this stereoselectivity likely derive from the unfavorability of formation of (*E*)-MAC over formation of (*Z*)-MAC. Similar control over the stereoselectivity of β-hydride elimination was observed during the intramolecular hydrosilylation of olefins catalyzed by [Rh((*S*)-BINAP)(acetone)$_2$](ClO$_4$).[21] We note that it is possible that elimination of the *pro-S*-β-hydride does occur within (S_{C_α})-**1**, but the resulting (*E*)-MAC does not dissociate from ruthenium but rather reinserts into the ruthenium−hydride bond to regenerate (S_{C_α})-**1**. The stoichiometric deuteriolysis of (S_{C_α})-**1** is mute on this point because β-hydride elimination within (S_{C_α},R_{C_β})-β-d_1-**1** will be of no net consequence if the resulting (*E*)-MAC-β-d_1 reinserts into the ruthenium−hydride bond without prior to olefin dissociation. We find it unlikely, however, that (*Z*)-MAC will dissociate from ruthenium but (*E*)-MAC will not.

The most likely explanation for formation of the other minor products of the stoichiometric deuteriolysis, (*R*,*R*)-MACH$_2$-β-d_1 (6%) and MACH$_2$ (~2%), is solvolysis of the ruthenium−carbon bonds in (S_{C_α},R_{C_β})-β-d_1-**1** and (S_{C_α})-**1**, respectively, by adventitious water or by acetone.[22]

We conclude from the predominant formation of (*R*,*R* and *S*,*S*)-MACH$_2$-α,β-d_2 by the stoichiometric deuteriolysis of (S_{C_α})-**1** that olefin coordination, olefin−hydride insertion, and their reverse transformations are rapid relative to the hydrogenolysis of the ruthenium−carbon bond under these reaction conditions (which include a build up of MeCN in solution as the reaction proceeds). We also conclude that β-hydride elimination within (S_{C_α})-**1** is highly stereoselective, favoring formation of the more stable olefin isomer, (*Z*)-MAC. The catalytic deuteration of (*E*)-MAC and (*Z*)-MAC were carried out to investigate the stereoselectivity of the catalytic hydrogenation.

Stereoselectivity and Regioselectivity of the Catalytic Hydrogenation. The catalytic deuteration of (*Z*)-MAC in acetone generated (*R*,*R* and *S*,*S*)-MACH$_2$-α,β-d_2 as the only detectable diastereomers in 92% ee (*R*,*R*) (eq 7). The net cis addition of dideuterium gas

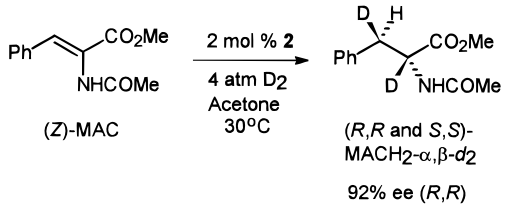

(7)

across (*Z*)-MAC, although consistent with the stereochemistry of the stoichiometric deuteriolysis of (S_{C_α})-**1**, it is also consistent with any mechanism involving olefin−hydride insertion followed by reductive elimination of a carbon−hydrogen bond. The net cis addition implies, however, that if the catalytic hydrogenation proceeds through (S_{C_α})-**1** or a similar species, any β-hydride elimination which occurred was highly stereoselective, favoring formation of (*Z*)-MAC.

The catalytic hydrogenation and deuteration of (*E*)-MAC were carried out to investigate if formation of (S_{C_α})-**1** (Figure 1) or of a similar species is reversible during the catalytic hydrogenation (eq 4). The catalytic hydrogenation of (*E*)-MAC in acetone produced MACH$_2$ in 91% ee (*R*), which is similar to the ee for hydrogenation of (*Z*)-MAC (92% (*R*)). The similar ee's indicate that both hydrogenations proceed through the same olefin geometry, implying that the hydrogenation of (*E*)-MAC proceeds via a rapid prior isomerization to (*Z*)-MAC.[23]

The catalytic deuteration of (*E*)-MAC was carried out to determine if olefin isomerization occurs prior to formation of MACH$_2$. Insertion of (*E*)-MAC into a ruthenium−deuterium bond with placement of ruthenium at the α-carbon followed by β-elimination favoring the (*Z*) isomer would form (*Z*)-MAC-β-d_1 with deuterium at the β-position. Deuteration of (*Z*)-MAC-β-d_1 would then lead to MACH$_2$-α,β,β-d_3. Figure 3 shows the distribution of isotopomers produced by the catalytic deuteration of (*E*)-MAC in acetone (MACH$_2$-α,β,β-d_3, 69%; (*R*,*R* and *S*,*S*)-MACH$_2$-α,β-d_2, 20%; MACH$_2$-β,β-

(20) Assuming, for the sake of argument that β-hydride elimination did not occur during the deuteration of (*E*)-MAC, the absolute configuration of MACH$_2$-α,β,β-d_3 resulting from deuteration of (*E*)-MAC-β-d_1 would depend on the enantioselectivity of the catalyst toward (*E*)-MAC.

(21) (a) Bergens, S. H.; Noheda, P.; Whelan, J.; Bosnich, B. *J. Am. Chem. Soc.* **1992**, *114*, 2121−2128. (b) Bergens, S. H.; Noheda, P.; Whelan, J.; Bosnich, B. *J. Am. Chem. Soc.* **1992**, *114*, 2128−2135.

(22) Other explanations include reaction via the small amount of HD gas generated by reaction of **2** with D$_2$ and olefin−hydride insertion of (Z)-MAC into **2** via the opposite regiochemistry (with ruthenium at the β-olefinic carbon and hydrogen at the α-olefinic carbon) followed by deuteriolysis of the ruthenium−carbon bond. Reaction with HD gas cannot be ruled out, but it is unlikely because the HD gas generated by reaction of **2** with D$_2$ amounts to ~2% of the D$_2$ in the reactor and because the concentration of **2** relative to 2-*d* is probably quite low.

(23) Another possibility, which we do not rule out, is that the intrinsic face selectivity of the hydrogenation toward (*E*)-MAC and (*Z*)-MAC are the same.

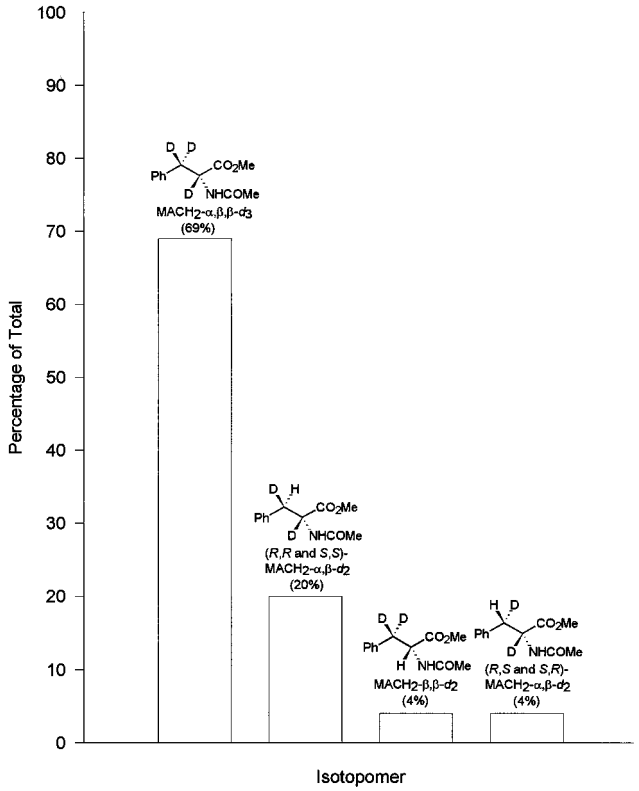

Figure 3. The distribution of $MACH_2$-d_n isotopomers from the catalytic deuteration of (*E*)-MAC using **2** as catalyst in acetone. The isotopomers (*R*,*R* and *S*,*S*)-$MACH_2$-β-d_1 and $MACH_2$-α-d_1 (combined 3% of total mixture) are not shown.

d_2, 4%; (*R*,*S* and *S*,*R*)-$MACH_2$-α,β-d_2, 4%; (*R*,*R* and *S*,*S*)-$MACH_2$-β-d_1, ∼1%; and $MACH_2$-α-d_1, ∼2%). The combined ee of the products was 92% (*R*,*R* and *R*). $MACH_2$-α,β,β-d_3 amounted to 69% of the product mixture, which is strong evidence that prior isomerization of (*E*)-MAC to (*Z*)-MAC occurred during the catalytic deuteration. Scheme 4 shows the sequence of steps that accounts for this distribution of isotopomers via a rapid formation of (S_{C_α})-**1** or a related species which is reversible via a stereoselective β-hydride elimination, as shown for the stoichiometric deuteriolysis of (S_{C_α})-**1**. Coordination of (*E*)-MAC to **2**-*d* through the *re*-face or the *si*-face followed by olefin−hydride insertion generates (R_{C_α},R_{C_β})- or (S_{C_α},S_{C_β})-β-d_1-**1**, respectively (Scheme 4, upper left). Stereoselective β-hydride elimination within (R_{C_α},R_{C_β})-β-d_1-**1** or (S_{C_α},S_{C_β})-β-d_1-**1** to favor formation of (*Z*)-MAC followed by olefin dissociation generates (*Z*)-MAC-β-d_1, **2**, and subsequently **2**-*d* (by reaction of **2** with dideuterium (eq 6)). Deuteration of (*Z*)-MAC-β-d_1 using **2**-*d* as the catalyst generates $MACH_2$-α,β,β-d_3, the predominant product of the catalytic deuteration (69%, Scheme 4, upper right). An initial isomerization of (*E*)-MAC to (*Z*)-MAC via the same sequence of steps likely accounts for the catalytic hydrogenations of (*E*)-MAC and (*Z*)-MAC occurring with similar ee's. The formation of $MACH_2$-α,β,β-d_3 is strong evidence that at least 69% of (*E*)-MAC underwent isomerization to (*Z*)-MAC-β-d_1 via the reversible formation of (S_{C_α})-**1** or of a structurally related species during the catalytic reaction (although not necessarily as part of the catalytic cycle). Further, a rapid and reversible formation of (S_{C_α})-**1** via stereoselective β-hydride elimination is also consistent with formation of (*R*,*R* and *S*,*S*)-$MACH_2$-α,β-d_2 as the only detectable product from the catalytic deuteration of (*Z*)-MAC (eq 7).

The amount of $MACH_2$-α,β,β-d_3 in the product mixture (69%) is the lower limit to the extent of isomerization of (*E*)-MAC to (*Z*)-MAC prior to deuteration because we propose that (*R*,*R* and *S*,*S*)-$MACH_2$-α,β-d_2 (20%) also arose from such a process. As discussed previously, (*R*,*R* and *S*,*S*)-$MACH_2$-α,β-d_2 (20%) results from a net cis addition of dideuterium to (*Z*)-MAC (eq 7). We believe deuterium-free (*Z*)-MAC was produced during the catalytic deuteration of (*E*)-MAC through reaction of (*E*)-MAC with **2**, which resulted from the stereoselective β-hydride elimination within (R_{C_α},R_{C_β})-β-d_1-**1** or (S_{C_α},S_{C_β})-β-d_1-**1** (Scheme 4, top, and as discussed in the previous paragraph). It is reasonable to propose that rather than reacting with dideuterium gas to generate **2**-*d*, some of **2** reacted with (*E*)-MAC (which is in up to 50-fold excess under *catalytic* conditions) to generate a *deuterium-free* diastereomer of (S_{C_α})-**1** or structurally related species (Scheme 4, middle). (*Z*)-Stereoselective β-hydride elimination followed by substrate dissociation will generate **2** and deuterium-free (*Z*)-MAC. Deuteration of (*Z*)-MAC then generates (*R*,*R* and *S*,*S*)-$MACH_2$-α,β-d_2 (20%).

Scheme 5 shows another conceivable route to formation of deuterium-free (*Z*)-MAC during the catalytic deuteration of (*E*)-MAC.[3h,i] In this sequence, **2**-*d* activates the N−H bond of (*E*)-MAC to generate the corresponding amido−allyl complex **5**. $\pi-\sigma-\pi$ rearrangement through formation of a ruthenium−carbon σ bond at the β-position would form the amido−allyl complex **5′**, which could eliminate (*Z*)-MAC-*N*-*d*. Deuteration of (*Z*)-MAC-*N*-*d* will generate (*R*,*R* and *S*,*S*)-$MACH_2$-α,β,*N*-d_3. As mentioned previously,[17] varying amounts of product deuterated at nitrogen were observed in all reactions carried out under dideuterium gas in acetone solution. Control experiments show that **2** catalyzes the H−D exchange between dideuterium and the N−H group of $MACH_2$ and (by extension) presumably also of MAC. The formation of N−D products by the catalytic reaction under dideuterium gas, therefore, cannot be used as direct evidence for involvement of amido−allyl (**5**, **5′**) or related species in the catalytic hydrogenation. We have no experimental evidence that *conclusively* distinguishes between reaction of **2** with (*E*)-MAC to form (S_{C_α})-**1** (Scheme 4, middle) or formation of an amido−allyl species (Scheme 5, **5** and **5′**) to account for formation of (*Z*)-MAC during the catalytic deuteration. Evidence against an amido−allyl species, however, is that little, if any, H−D exchange between nitrogen and the α- or β-carbon centers occurs during the catalytic deuteration of (*Z*)-MAC in methanol solvent (*vide infra*, eq 8). It is reasonable to expect amido−allyl species such as **5** and **5′** to some extent undergo deuteride addition to the β-carbon-forming species such as **6** and **6′** (Scheme 5). Among other things, these sequences of steps would allow H−D exchange between nitrogen and the β-carbon. The lack of an observable amount of such exchange during the catalytic deuteration of (*Z*)-MAC in methanol favors formation of (*Z*)-MAC via reaction of **2** with (*E*)-MAC (Scheme 4, middle) over an amido−allyl route.

The major product of the catalytic deuteration of (*E*)-MAC, $MACH_2$-α,β,β-d_3 (69%), resulted from formation

Scheme 4

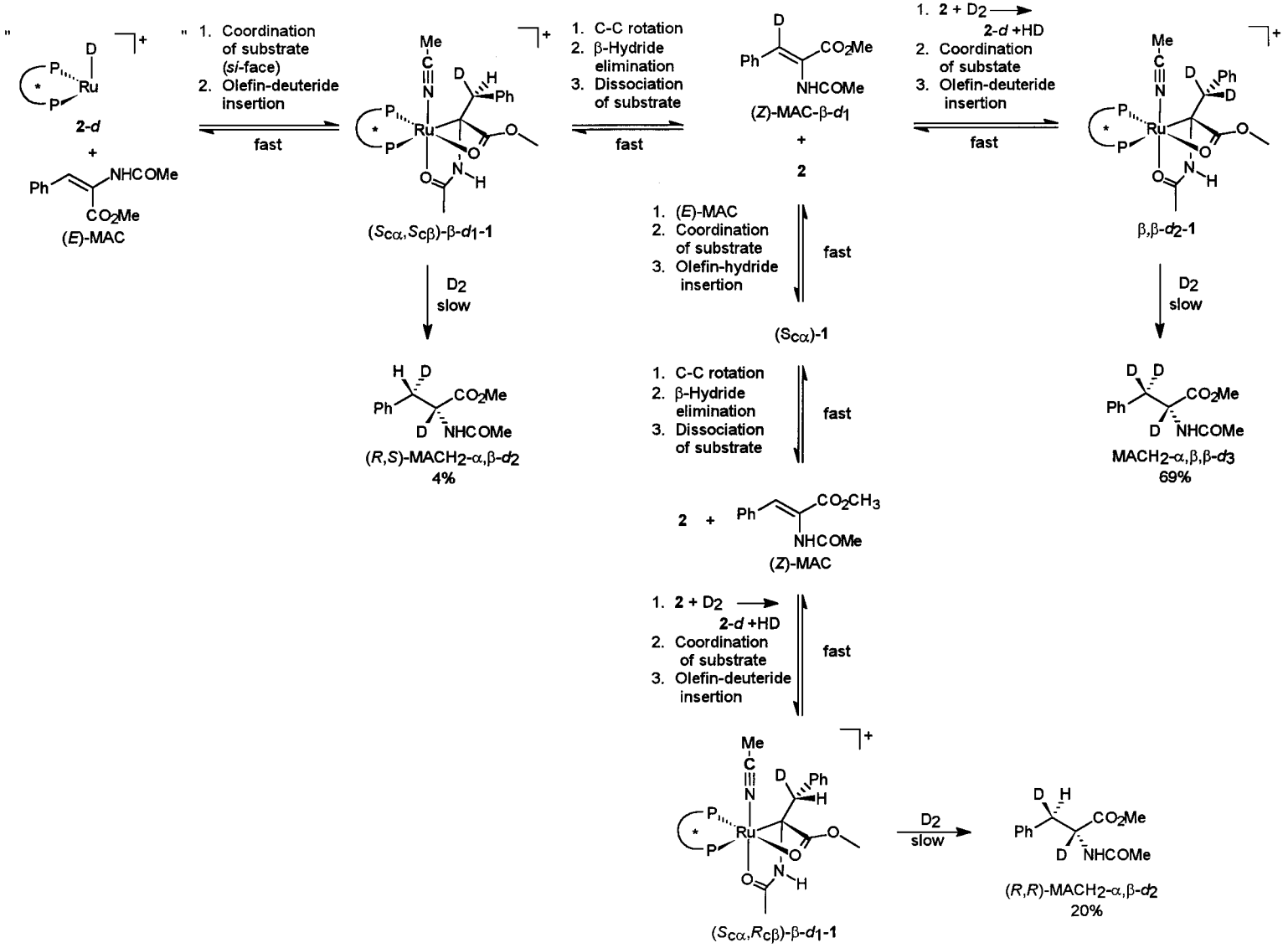

Scheme 5

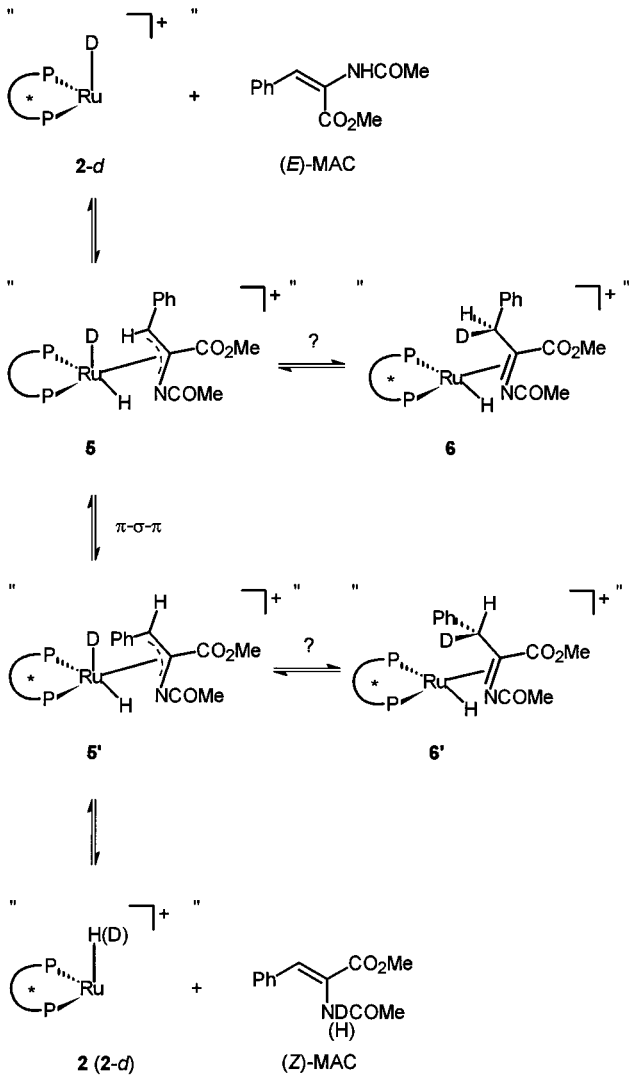

of (S_{C_α})-**1** or a related species via a rapid net cis addition of ruthenium and deuterium across the carbon−carbon double bond, followed by a rapid stereoselective β-hydride elimination. We propose that it is likely that a further 20% of the product, (*R*,*R* and *S*,*S*)-$MACH_2$-α,β-d_2, also resulted from such a sequence of steps. We therefore conclude from the product distributions of the catalytic deuteration of (*E*)-MAC and (*Z*)-MAC in acetone that the sum of the stereoselectivities and regioselectivities of the reversible formation of (S_{C_α})-**1** and its hydrogenolysis equals the overall stereoselectivity and regioselectivity of the catalytic hydrogenation.

One of the minor products of the catalytic deuteration of (*E*)-MAC, (*R*,*S* and *S*,*R*)-$MACH_2$-α,β-d_2 (4%), likely arose from the direct deuteration of (*E*)-MAC without prior isomerization to (*Z*)-MAC (Scheme 4, left, deuteriolysis of (S_{C_α},S_{C_β})-β-d_1-**1**)). Of the remaining minor products of the catalytic deuteration of (*E*)-MAC, we speculate that $MACH_2$-α-d_1 (~2%) resulted from deuteriolysis of **1** or from reaction of HD gas with (*E*)-MAC catalyzed by **2**. (*R*,*R* and *S*,*S*)-$MACH_2$-β-d_2 (1%) and $MACH_2$-β,β-d_2 (4%) likely arose from solvolysis of the ruthenium−carbon bond in (R_{C_α},S_{C_β} and S_{C_α},R_{C_β})-β-d_1-**1** and β,β-d_2-**1**, respectively by adventitious water.

Methanol as the Solvent. The catalytic deuteration of (*Z*)-MAC was carried out in methanol to determine the ratio of solvolysis to hydrogenolysis during catalysis in this protic solvent. As shown in eq 8, the product ratio was (*R*,*R* and *S*,*S*)-$MACH_2$-α,β-d_2, 96%; and (*R*,*R* and *S*,*S*)-$MACH_2$-β-d_1, 4% (combined ee = 89% (*R*,*R*)).

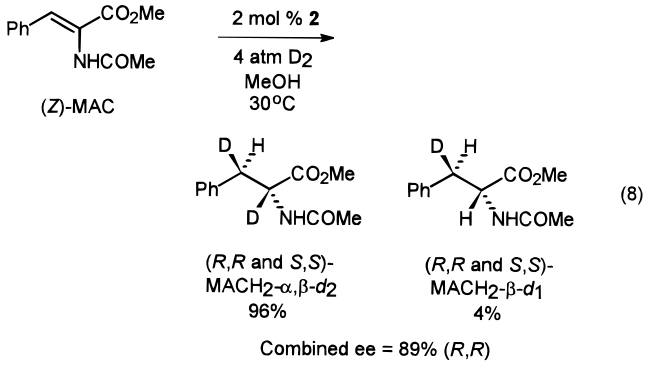

(8)

The low percentage of $MACH_2$ with hydrogen at the α-position shows that solvolysis of a ruthenium−carbon bond is *not* a major pathway of the catalytic hydrogenation in methanol. The 96% relative abundance of (*R*,*R* and *S*,*S*)-$MACH_2$-α,β-d_2 also shows that little H−D exchange occurs between nitrogen and the α- and β-carbon centers during the catalytic hydrogenation. This is evidence against involvement of an amido−allyl (Scheme 5, **5** or **5′**) or related species in the catalytic cycle. We note that although the catalyst does effect H−D exchange between dideuterium and the N−H group of $MACH_2$ and (by extension) likely of (*Z*)-MAC, any deuterium substitution at nitrogen that arose from such a process would immediately H−D exchange with the methanol solvent, effectively maintaining a proton at nitrogen throughout the catalytic hydrogenation.

The stoichiometric hydrogenolysis of (S_{C_α})-**1** slowed as the reaction proceeded in acetone (eq 2) but went to completion in methanol. In methanol solvent, the rate of the stoichiometric hydrogenolysis was similar to the turnover frequency of the catalytic hydrogenation.[6] The stoichiometric deuteration of (S_{C_α})-**1** was carried out in methanol to investigate the origins of this discrepancy in behavior between acetone and methanol solvents. Figure 4 shows the distribution of organic products from the stoichiometric deuteriolysis of (S_{C_α})-**1** in methanol (eq 9; (*R*,*R* and *S*,*S*)-$MACH_2$-α,β-d_2, 58%; $MACH_2$-α-d_1, 5%; (*R*,*R* and *S*,*S*)-$MACH_2$-β-d_1, 16%; and $MACH_2$, 21%). The combined ee was 85% (*R*,*R* and *R*), similar

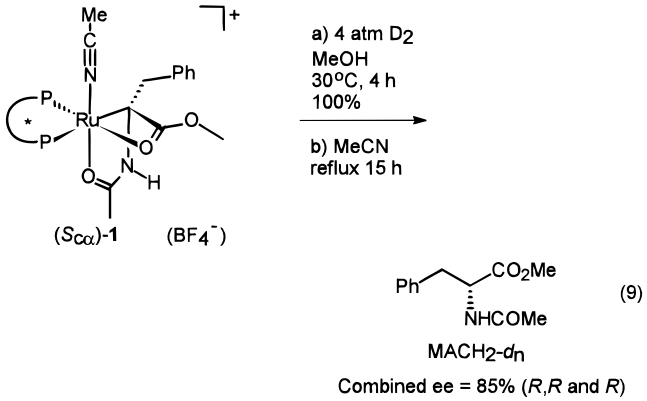

(9)

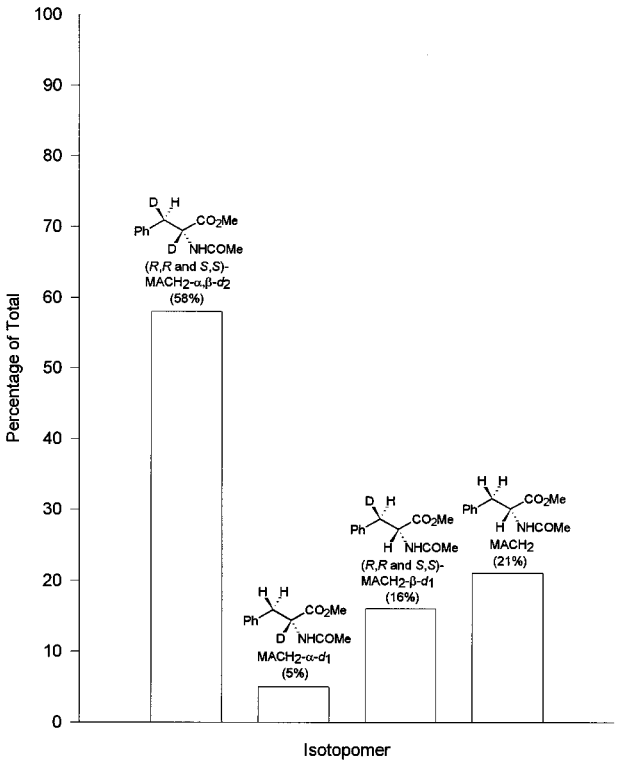

Figure 4. The distribution of $MACH_2$-d_n isotopomers from the deuteriolysis of ($S_{C\alpha}$)-**1** in methanol.

to the catalytic hydrogenation in methanol (87% (*R*)). Only the (*R*,*R*)- and (*S*,*S*)-diastereomers of $MACH_2$-α,*β*-d_2 were detected, showing that *β*-elimination within (S_{C_α})-**1** proceeds by the same stereoselectivity as that observed in acetone. The ratio of (*R*,*R* and *S*,*S*)-$MACH_2$-α,*β*-d_2 to $MACH_2$-α-d_1 (∼12:1) also indicates that the reversible formation of (S_{C_α})-**1** was faster than deuteriolysis of the ruthenium−carbon bond. The $MACH_2$ (21%) and (*R*,*R* and *S*,*S*)-$MACH_2$-*β*-d_1 (16%) resulted from solvolysis of the ruthenium−carbon bond in (S_{C_α})-**1** and in (S_{C_α},R_{C_β})-*β*-d_1-**1**, respectively. The total amount of $MACH_2$ and (*R*,*R* and *S*,*S*)-$MACH_2$-*β*-d_1 (37%) is likely a direct indication of the amount of solvolysis that occurred under these conditions, because control experiments show that **2** does not catalyze the H−D exchange between dideuterium gas and methanol at an appreciable rate. At this stage, we conclude that the similarity of rates for the stoichiometric hydrogenolysis in methanol and for the catalytic hydrogenation in methanol is coincidental and is not of mechanistic significance.

Unlike the reaction in acetone solution, the stoichiometric hydrogenolysis of (S_{C_α})-**1** in methanol solution was not significantly inhibited, even by the addition of a 20-fold excess of MeCN. The reasons why the stoichiometric hydrogenation of (S_{C_α})-**1** is not appreciably inhibited by MeCN in methanol solution likely relate to the ability of (S_{C_α})-**1** to undergo solvolysis in methanol to generate $MACH_2$. As solvolysis likely proceeds by protonation of the ruthenium center in (S_{C_α})-**1**, we suspect that solvolysis is not significantly inhibited by MeCN because protonation of a metal center does not require a vacant coordination site.[24] Whatever their origins, the relative susceptibilities of the stoichiometric hydrogenolysis of (S_{C_α})-**1** to inhibition by MeCN in acetone and in methanol solution do not appreciably influence the catalytic hydrogenation as the turnover frequency is higher in acetone than in methanol, at least 980 turnovers can be achieved in acetone, and the catalytic hydrogenation in methanol solution *does not* proceed via solvolysis of a ruthenium−carbon bond.

Conclusions

This work is the first mechanistic study of a ruthenium−BINAP-catalyzed hydrogenation to be complimented by a solid-state structure of a possible intermediate with a prochiral substrate group bonded to ruthenium. We conclude from the results of this study that the stereoselectivities and the regioselectivities of the rapid reversible formation of (S_{C_α})-**1** and its conversion to $MACH_2$ (via irreversible hydrogenolysis of the ruthenium−carbon bond) summate to give the stereoselectivity and regioselectivity of the catalytic hydrogenation. We also conclude that solvolysis of the ruthenium−carbon bond is a minor (<4%) pathway of the catalytic hydrogenation in methanol solvent and that the presence of MeCN in the system does not contribute to the enantioselection of the catalytic reaction. Although (S_{C_α})-**1** is the only detectable species in solution during the catalytic reaction at room temperature, the data from this study do not distinguish between whether (S_{C_α})-**1** is a catalytic intermediate or a species in equilibrium with the true catalytic intermediate. Further, a direct comparison between the stoichiometric and catalytic rate data are complicated by both the build up of MeCN, which occurs in solution during the stoichiometric hydrogenolysis, and by the ability of (S_{C_α})-**1** to undergo solvolysis in methanol. Both of these processes do not occur during the catalytic hydrogenation. A kinetic study to investigate these issues is underway in our laboratories.

Experimental Section

General Considerations. All glassware was sequentially treated with ethanolic ammonia solution and acetone and dried overnight in an oven at 120 °C before use. Reactions involving organometallic compounds were conducted under an atmosphere of dry argon gas (Praxair, 99.998%) using standard Schlenk techniques. Organometallic products were isolated in a drybox filled with dinitrogen gas (Praxair, 99.998%) and stored at −30 °C for prolonged periods.

Physical and Spectral Measurements. NMR spectra were recorded using Bruker AM-400 (^{1}H at 400.1 MHz, ^{2}H at 61.4 MHz, ^{13}C at 100.6 MHz, and ^{31}P at 161.9 MHz) and Bruker AM-R-300 (^{13}C CP/MAS at 75.5 MHz) spectrometers. The chemical shifts for ^{1}H, ^{2}H, and ^{13}C were measured relative to external TMS and referenced to residual solvent signals; those signals for ^{31}P were measured relative to an 85% H_3PO_4 external reference. Routine electron-impact high-resolution mass spectrometry (HRMS (EI)) of organic compounds were performed on a Kratos MS50 spectrometer. Mass spectrometric analyses of organometallic compounds were performed by positive-mode electrospray ionization (ESI-MS (pos)) on a Micromass ZabSpec Hybrid Sector-TOF spectrometer. Calculated *m*/*z* values refer to the isotopes ^{12}C, ^{1}H, ^{14}N, ^{16}O, ^{31}P, and ^{102}Ru. Optical rotations were measured with a Perkin-Elmer 241 polarimeter at 589 nm using 1.0 dm cells. Mi-

(24) (a) Crabtree, R. H.; Quirk, J. M.; Fillebeen-Khan, T.; Morris, G. E. *J. Organomet. Chem.* **1979**, *181*, 203−212. (b) Ashworth, T. V.; Singleton, J. E.; de Waal, D. J. A.; Louw, W. J.; Singleton, E.; van der Stok, E. *J. Chem. Soc., Dalton Trans.* **1978**, 340−347. See also, electrophilic attack of $HgBr_2$ on Cp*Os(CO)(PMe_2Ph)Me: Sanderson, L. J.; Baird, M. C. *J. Organomet. Chem.* **1986**, *307*, C1−C4.

croanalyses were performed at the University of Alberta Microanalysis Laboratory.

Materials. All solvents (reagent grade) were purchased from Caledon and Fisher Scientific, except deuterated solvents (99.8−99.9% D) which were purchased from Cambridge Isotope Laboratories. Acetone (3 Å molecular sieves), acetone-d_6 (3 Å molecular sieves), acetonitrile (phosphorus pentoxide), diethyl ether (lithium aluminum hydride), methanol (magnesium methoxide), methanol-d_4 (magnesium methoxide-d_6), methylene chloride (calcium hydride), methylene chloride-d_2 (calcium hydride), tetrahydrofuran (potassium benzophenone ketyl), and tetrahydrofuran-d_8 (potassium) were distilled from the appropriate drying agents under an atmosphere of argon gas prior to use. All other solvents were used as received. Dihydrogen gas (Praxair, 99.99%) was passed through an Alltech Oxy-Trap to remove trace amounts of oxygen, whereas dideuterium gas (Aldrich, 99.8%; Praxair, 99.7%) was used as received. α-Acetamidocinnamic acid was purchased from Aldrich and recrystallized 5 times from ethanol/hexanes before use. (*Z*)-Methyl α-acetamidocinnamate was prepared by the esterification of α-acetamidocinnamic acid using diazomethane.[25,26] (*Z*)-Methyl-4-benzaloxazolone,[27] (*E*)-methyl α-acetamidocinnamate,[26] and [Ru((*R*)-BINAP)(1−3;5−6-η-C_8H_{11})(MeCN)]-(BF_4)[7] were prepared using established procedures. (*rac*)-*N*-Acetylphenylalanine methyl ester was obtained by hydrogenating (*Z*)-methyl α-acetamidocinnamate using [Rh(η^4-norbornadiene)(1,2-bis(diphenylphosphino)ethane)](ClO_4)[28] as the catalyst. All other materials were purchased from Aldrich with the exception of (*S*)-*N*-acetylphenylalanine methyl ester (Serva) and Florisil (60−100 mesh, Fisher Scientific).

(*Z*)-Methyl-d_3 α-Acetamidocinnamate. To a stirred suspension of (*Z*)-methyl-4-benzaloxazolone (459.7 mg, 2.46 mmol) in benzene (5 mL) at room temperature, a ∼1 M sodium methoxide solution (prepared from sodium (73.8 mg, 3.21 mmol) and methanol (3 mL)) was added. The resulting pale yellow solution was allowed to stir for 5 min, after which the solution was acidified with aqueous 0.1 M HCl. The slightly opaque benzene layer was extracted with methylene chloride (3 × 10 mL) and washed with water (3 × 20 mL). The organic layer was dried over anhydrous magnesium sulfate, filtered, and evaporated to yield 226.4 mg (41%) of (*Z*)-Methyl-d_3 α-acetamidocinnamate. NMR spectroscopic data (50 °C): ^{1}H (400.1 MHz, $CDCl_3$) δ 2.00 (br s, 3H, NHCOCH_3), 7.30 (m, 5H), 7.45 (br s, 2H); ^{2}H{^{1}H} (61.4 MHz, $CHCl_3$) δ 3.80 (s, CO_2CD_3); ^{13}C{^{1}H} (100.6 MHz, $CDCl_3$) δ 22.8 (br s, NHCO*C*H_3), 124.9 (quaternary), 128.5 (methine), 129.4 (methine), 129.7 (methine), 132.5 (br s, methine), 133.7 (quaternary), 165.9 (CO_2CH_3), 169.4 (br s, NH*C*OCH$_3$). The methoxy ^{13}C resonance appears at δ 52.4 ppm for (*Z*)-methyl α-acetamidocinnamate. HRMS (EI, direct insert) *m*/*z* 222.1083 (M^+, exact mass calcd for $C_{12}H_{10}D_3NO_3$ 222.1084). Anal. Calcd for $C_{12}H_{13}NO_3$: C, 65.74; H, 5.98; N, 6.39. Found: C, 65.39; H, 5.93, N, 6.19.

[Ru((*R*)-BINAP)((*S*)-MACH)(MeCN)](BF$_4$) ((S_{C_α})-1). [Ru((*R*)-BINAP)(1−3;5−6-η-C_8H_{11})(MeCN)](BF_4) (547.5 mg, 0.571 mmol) was partially dissolved in acetone (20.0 mL) under an atmosphere of dry argon gas and subjected to 3 freeze−pump−thaw cycles. The reactor was backfilled with dihydrogen gas (20 psig) at room temperature and vigorously shaken for 10 min to generate a clear, dark orange solution. This extremely air-sensitive solution was subjected to 2 freeze−pump−thaw cycles and backfilled with argon gas. To this solution at room temperature, an acetone solution (5.0 mL) of (*Z*)-methyl α-acetamidocinnamate (125.2 mg, 0.571 mmol) was added. The resulting dark amber solution was shaken, and the solvent was removed under reduced pressure to give a yellow solid discolored by a brown residue. Dropwise addition of diethyl ether (80 mL) to a methylene chloride solution (2.5 mL) of the product afforded a yellow powder. The product was filtered off, washed with diethyl ether (5 × 10 mL), and dried under dynamic vacuum (16 h) to yield 534.1 mg (87%) of (S_{C_α})-**1**. NMR spectroscopic data for (S_{C_α})-**1** (CD_2Cl_2, 25 °C): ^{1}H (400.1 MHz) δ 1.71 (s, 3H, CH_3CN), 1.95 (s, 3H, NHCOCH_3), 2.70 (dd, $^2J_{H-H}$ = 14.0 Hz, $^4J_{P-H}$ = 4.5 Hz, 1H, *pro*-*R*-CH_2Ph), 3.98 (s, 3H, CO_2CH_3), 4.15 (d, $^2J_{H-H}$ = 14.0 Hz, 1H, *pro*-*S*-CH_2Ph), 5.87 (br d, $^5J_{P-H}$ = 2.7 Hz, 1H, N*H*COCH$_3$), 6.40−8.00 (aromatic); ^{31}P{^{1}H} (161.9 MHz) δ 33.6 (d, $^2J_{P-P}$ = 23.8 Hz, 1P), 59.7 (d, $^2J_{P-P}$ = 23.8 Hz, 1P); ^{13}C{^{1}H} (100.6 MHz) δ 4.7 (s, *C*H$_3$CN), 20.9 (s, NHCO*C*H$_3$), 38.5 (s, *C*H$_2$Ph), 53.3 (s, CO_2CH_3), 67.3 (dd, $^2J_{C-P_{trans}}$ = 42.2 Hz, $^2J_{C-P_{cis}}$ = 3.9 Hz, Ru−*C*), 126−143 (aromatic and CH_3CN), 160.8* (d, $^3J_{C-P}$ = 3.3 Hz), 179.7* (d, $^3J_{C-P}$ = 7.0 Hz); ^{13}C CP/MAS (75.5 MHz) δ 6, 21, 39, 56, 69, 128, 134, 161, 181. ESI-MS (pos) *m*/*z* 985.2 (($M - BF_4$)$^+$, exact mass calcd for $C_{58}H_{49}N_2O_3P_2Ru$ 985.2). Anal. Calcd for $C_{58}H_{49}BF_4N_2O_3P_2Ru$: C, 64.99; H, 4.61; N, 2.61. Found: C, 63.85; H, 4.65; N, 2.86. The signals marked with an asterisk are those of the amide carbonyl and ester carbonyl carbons. Isotopic-labeling experiments have not been conducted to unambiguously assign these signals.

[Ru((*R*)-BINAP)(H)(η^6-(*rac*)-MACH$_2$)](BF$_4$). (*rac*)-*N*-Acetylphenylalanine methyl ester (15.1 mg, 0.068 mmol) and [Ru((*R*)-BINAP)(1−3;5−6-η-C_8H_{11})(MeCN)](BF_4) (65.5 mg, 0.068 mmol) were dissolved in acetone (8.0 mL) under an atmosphere of argon gas and subjected to 3 freeze−pump−thaw cycles. The reactor was backfilled with dihydrogen gas (20 psig) at room temperature and shaken 10 min. The resulting solution was concentrated (∼1 mL) under reduced pressure. Addition of diethyl ether (∼100 mL) followed by filtration afforded a yellow powder. The product was washed with diethyl ether (5 × 10 mL) and dried under dynamic vacuum (24 h) to yield 39.4 mg (56%) of [Ru((*R*)-BINAP)(H)(η^6-(*rac*)-MACH$_2$)](BF_4). A reaction mixture monitored by ^{1}H and ^{31}P NMR spectroscopy confirmed that the two diastereomeric complexes were formed in quantitative yield. The individual diastereomer, [Ru((*R*)-BINAP)-(H)(η^6-(*S*)-MACH$_2$)](BF_4), was prepared using (*S*)-*N*-acetylphenylalanine methyl ester in a manner analogous to that described above. NMR spectroscopic data (CD_2Cl_2, 25 °C) for (R_{BINAP},S_{MACH_2}) diastereomer: ^{1}H (400.1 MHz) δ −9.14 (dd, $^2J_{P-H}$ = 40.3 Hz, $^2J_{P-H}$ = 29.3 Hz, 1H, Ru−*H*), 1.83 (s, 3H, NHCOCH_3), 2.51 (dd, $^2J_{H_\beta-H_{\beta'}}$ = 13.8 Hz, $^3J_{H_\alpha-H_\beta}$ = 5.0 Hz, 1H, $C_6H_5CH_2CH$ (H_β)), 2.82 (dd, $^2J_{H_\beta-H_{\beta'}}$ = 13.8 Hz, $^3J_{H_\alpha-H_{\beta'}}$ = 7.8 Hz, 1H, $C_6H_5CH_2CH$ ($H_{\beta'}$)), 3.62 (s, 3H, CO_2CH_3), 4.40 (d, $^3J_{H-H}$ = 6.1 Hz, 1H, $C_6H_5CH_2CH$), 4.47 (d of app t, $^3J_{H_\alpha-H_{\beta'}}$ = $^3J_{H_\alpha-H_{N-H}}$ = 7.8 Hz, $^3J_{H_\alpha-H_\beta}$ = 5.0 Hz, 1H, $C_6H_5CH_2CH$ (H_α)), 4.55 (app t, $^3J_{H-H}$ = 6.1 Hz, 1H, $C_6H_5CH_2CH$), 5.45 (d, $^3J_{H-H}$ = 6.2 Hz, 1H, $C_6H_5CH_2CH$), 5.78 (app t, $^3J_{H-H}$ = 6.1 Hz, 1H, $C_6H_5CH_2CH$), 6.03 (app t, $^3J_{H-H}$ = 5.9 Hz, 1H, $C_6H_5CH_2CH$), 6.15−8.20 (BINAP); ^{31}P{^{1}H} (161.9 MHz) δ 50.4 (d, $^2J_{P-P}$ = 45.5 Hz, 1P), 51.5 (d, $^2J_{P-P}$ = 45.5 Hz, 1P). NMR spectroscopic data (CD_2Cl_2, 25 °C) for (R_{BINAP},R_{MACH_2}): ^{1}H (400.1 MHz) δ −9.06 (dd, $^2J_{P-H}$ = 36.0 Hz, $^2J_{P-H}$ = 33.6 Hz, 1H, Ru−*H*), 1.88 (s, 3H, NHCOCH_3), 2.56 (dd, $^2J_{H_\beta-H_{\beta'}}$ = 14.0 Hz, $^3J_{H_\alpha-H_\beta}$ = 8.0 Hz, 1H, $C_6H_5CH_2CH$ (H_β)), 2.98 (dd, $^2J_{H_\beta-H_{\beta'}}$ = 14.0 Hz, $^3J_{H_\alpha-H_{\beta'}}$ = 5.0 Hz, 1H, $C_6H_5CH_2CH$ ($H_{\beta'}$)), 3.62* (s, CO_2CH_3), 4.43* ($C_6H_5CH_2CH$ (H_α)), 4.89 (d, $^3J_{H-H}$ = 6.0 Hz, 1H, $C_6H_5CH_2CH$), 4.95 (app t, $^3J_{H-H}$ = 6.0 Hz, 1H, $C_6H_5CH_2CH$), 5.06 (d, $^3J_{H-H}$ = 6.0 Hz, 1H, $C_6H_5CH_2CH$), 5.60 (app t, $^3J_{H-H}$ = 6.0 Hz, 1H, $C_6H_5CH_2CH$), 6.03 (app t, $^3J_{H-H}$ = 6.0 Hz, 1H, $C_6H_5CH_2CH$), 6.00−8.20 (BINAP); ^{31}P{^{1}H} (161.9 MHz) δ 51.1 (d, $^2J_{P-P}$ = 45.0 Hz, 1P), 51.4 (d, $^2J_{P-P}$ = 45.0 Hz, 1P). ESI-MS (pos) *m*/*z* 946.2 (($M - BF_4$)$^+$, exact mass calcd for $C_{56}H_{48}NO_3P_2Ru$ 946.2).

(25) Casey, M.; Leonard, J.; Lygo, B.; Procter, G. *Advanced Practical Organic Chemistry*; Chapman & Hall: London, 1990; pp 70−73.
(26) Vineyard, B. D.; Knowles, W. S.; Sabacky, M. J.; Bachman, G. L.; Weinkauff, D. J. *J. Am. Chem. Soc.* **1977**, *99*, 5946−5952.
(27) Herbst, R. M.; Shemin, D. In *Organic Syntheses*; Blatt, A. H., Ed.; Wiley: New York, 1943; Collect. Vol. II, pp 1−3.
(28) Schrock, R. R.; Osborn, J. A. *J. Am. Chem. Soc.* **1971**, *93*, 2397−2407.

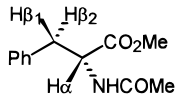

Figure 5. Designations used for the ABX spin system in the ^{1}H NMR spectrum of *N*-acetylphenylalanine methyl ester ($MACH_2$).

Anal. Calcd for $C_{56}H_{48}BF_4NO_3P_2Ru$: C, 65.12; H, 4.68; N, 1.36. Found: C, 64.39; H, 4.67; N, 1.68. Signals marked with an asterisk are overlapped by resonances of the (R_{BINAP},S_{MACH_2}) diastereomer.

General Procedure for Catalytic Hydrogenations. A glass pressure reactor (Lab Glass) was employed for hydrogenation reactions where the pressure of dihydrogen gas was ≤4 atm. For reactions requiring elevated pressures, a Parr cell-disruption bomb was used. In general, the appropriate pressure reactor was charged with substrate and catalyst (2 mol %) under an atmosphere of argon gas. The reaction vessel was flushed with dihydrogen gas and its contents dissolved in the appropriate deoxygenated solvent ([catalyst] = 2.6 mM). The reactor was pressurized (dynamic pressure)/heated to the desired levels and allowed to react for, typically, 48 h while stirring at 1100 rpm. Pressures were quoted as gauge pressure plus 1 atm. After complete conversion of reactant to product (confirmed by ^{1}H NMR spectroscopy and HRMS (EI)), the mixtures were evaporated under reduced pressure and the residues analyzed without further purification. Enantiomeric excesses were spectroscopically determined (^{1}H NMR) via chiral lanthanide shift reagent[29] (europium tris[3-(trifluoromethylhydroxymethylene)-(+)-camphorate] ((+)-Eu(tfc)$_3$)) in chloroform-*d*. The ratio of the methoxy signals (ca. 4 ppm; 1:1 for (*rac*)-*N*-acetylphenylalanine methyl ester) was used to quantify all enantiomeric excesses. In all cases, addition of (*S*)-*N*-acetylphenylalanine methyl ester caused a decrease in enantiomeric excess, indicating the absolute configuration of the major enantiomer was *R*. The catalyst residue was removed before polarimetry by passing an ethyl acetate solution of the reaction mixture through a column of Florisil. The enantiomeric excess and absolute configuration of the major enantiomer for this mixture were determined as described above and confirmed by the magnitude and the sign of the optical rotation,[3f] respectively, from polarimetry measurements.

General Procedure for Catalytic Deuterations. Reactions were performed in a manner similar to that described above with the following exceptions: (1) catalyst and substrate were dissolved in the appropriate solvent under an atmosphere of argon gas and subjected to 3 freeze−pump−thaw cycles prior to backfilling with dideuterium gas to the desired levels; and (2) the reactions were initially stirred under dynamic pressure (15 min), followed by static pressure for the remainder of the reaction. The relative proportions of isotopomers in the product mixture were determined via NMR spectroscopy and HRMS (EI). The ABX spin system in the ^{1}H NMR spectrum for the α- and *β*-protons of $MACH_2$ were assigned by comparison to the reported assignments established for *N*-acetylphenylalanine, the acid analogue of $MACH_2$ (Figure 5).[3h] Each isotopomer was quantified by integrating the signals of the protons and the methoxy signal as an internal reference. The amount of deuterium substitution at each position was obtained from ^{2}H{^{1}H} NMR spectra or deduced from the proton signals in the ^{1}H{^{2}H} NMR spectrum by subtraction if the signals in the ^{2}H{^{1}H} NMR spectrum overlapped and could not be deconvoluted. The presence of $MACH_2$-d_n (n = 0−3) were confirmed by the parent ion peaks in the mass spectrum. Of the eight possible isotopomers of $MACH_2$-d_n (n = 0−3), only seven were observed during the course of this investigation ($MACH_2$, (*R*,*R* and *S*,*S*)-$MACH_2$-*β*-d_1, $MACH_2$-α-d_1, $MACH_2$-*β*,*β*-d_2, (*R*,*S* and *S*,*R*)-$MACH_2$-α,*β*-d_2, (*R*,*R* and *S*,*S*)-$MACH_2$-α,*β*-d_2, and $MACH_2$-α,*β*,*β*-d_3). Of these seven isotopomers, six were identified and quantified by their ^{1}H{^{2}H} NMR spectra. The seventh isotopomer, $MACH_2$-*β*,*β*,*β*-d_3 was identified by HRMS (EI) and its relative amount was determined from the methoxy internal standard signal after subtracting the contributions from the other isotopomers. The ^{1}H{^{2}H} NMR spectrum of each isotopomer was in accord with line patterns predicted by substitution of the appropriate proton(s) by deuteron(s) in the assigned ABX system of $MACH_2$. For example, (*R*,*R* and *S*,*S*)-$MACH_2$-α,*β*-d_2 was idenified by its proton signal (δ 3.03 (s, 1H, H_{β_2})) which showed the absence of coupling to other protons and was shifted slightly upfield from the H_{β_2} signal for nondeuterated $MACH_2$.[30] Similarly, (*R*,*R* and *S*,*S*)-$MACH_2$-*β*-d_1 was identified by its proton signals (δ 3.03 (d, $^3J_{H_\alpha-H_{\beta2}}$ = 6.1 Hz, 1H, H_{β_2}), 4.85 (dd, $^3J_{H_\alpha-H_{NH}}$ = 7.8 Hz, $^3J_{H_\alpha-H_{\beta2}}$ = 6.1 Hz, 1H, H_α). The other isotopomers were identified in the same manner. Identifications were confirmed by ^{1}H{^{2}H, BB; ^{1}H, sel} NMR experiments. The combined enantiomeric excess and absolute configuration of the products for each mixture of isotopomers was determined using the aforementioned procedure. NMR spectroscopic data ($CDCl_3$, 25 °C) for *N*-acetylphenylalanine methyl ester ($MACH_2$): ^{1}H (400.1 MHz) δ 1.93 (s, 3H, NHCOCH_3), 3.03 (dd, $^2J_{H_{\beta1}-H_{\beta2}}$ = 13.9 Hz, $^3J_{H_\alpha-H_{\beta2}}$ = 6.1 Hz, 1H, H_{β_2}), 3.11 (dd, $^2J_{H_{\beta1}-H_{\beta2}}$ = 13.9 Hz, $^3J_{H_\alpha-H_{\beta1}}$ = 6.1 Hz, 1H, H_{β_1}), 3.68 (s, 3H, CO_2CH_3), 4.85 (d of app t, $^3J_{H_\alpha-H_{NH}}$ = 7.8 Hz, $^3J_{H_\alpha-H_{\beta1}}$ = $^3J_{H_\alpha-H_{\beta2}}$ = 6.1 Hz, 1H, H_α), 6.27 (br d, N*H*COCH$_3$), 7.08 (d, $^3J_{H-H}$ = 6.9 Hz, 2H, *o*-C_6H_5), 7.24 (m, 3H, *m*- and *p*-C_6H_5); ^{13}C{^{1}H} (100.6 MHz) δ 22.8 (NHCO*C*H$_3$), 37.6 (*C*H$_2$CH, C$_\beta$), 52.1 (CO_2CH_3), 53.1 (CH_2CH, C$_\alpha$), 126.9 (C_6H_5), 128.4 (C_6H_5), 129.0 (C_6H_5), 135.9 (*ipso*-C_6H_5), 169.7 (CO_2CH_3), 172.1 (NH*C*OCH$_3$).

General Procedure for Hydrogenolysis/Deuteriolysis of (S_{C_α})-1. Reactions were performed in a manner analogous to that described above for catalytic hydrogenations/deuterations with the exception that [(S_{C_α})-**1**] = 10 mM. Typical reaction times were 4 (in methanol) and 24 h (in acetone), after which all volatiles were removed under reduced pressure. The remaining residue was refluxed in acetonitrile under argon gas overnight (∼15 h), followed by evaporation under reduced pressure. The solid residue was washed with ethyl acetate, and the solution was passed through a column of Florisil to remove residual ruthenium−BINAP species. Removal of the solvent on a rotary evaporator yielded pure *N*-acetylphenylalanine methyl ester, which was analyzed without further purification. Enantiomeric excesses and the distributions of deuterium were determined using the aforementioned procedures.

Substrate Equilibrium with (S_{C_α})-1. In a 5-mm NMR tube, (*Z*)-methyl-d_3 α-acetamidocinnamate (5.8 mg, 2.6 × 10^{-5} mol) and (S_{C_α})-**1** (9.9 mg, 9.2 × 10^{-6} mol) were dissolved in a mixture of CD_2Cl_2 (∼0.1 mL, used to ensure complete dissolution of (S_{C_α})-**1**) and acetone-d_6 (∼0.5 mL). The sample was immediately placed in a thermostated NMR probe (T = 35 °C) and monitored by ^{1}H NMR spectroscopy. The extent of the reaction was determined by the ratio of the methoxy signals of (S_{C_α})-**1** and (*Z*)-MAC (singlets at 4.0 and 3.8 ppm, respectively) using a benzylic proton of (S_{C_α})-**1** as the internal standard (doublet at 4.2 ppm). ^{31}P NMR spectroscopy indicated the only ruthenium species present in the reaction mixture was (S_{C_α})-**1** and (S_{C_α})-**1**-Me-d_3.

Acknowledgment. This work was financially supported by the Natural Sciences and Engineering Research Council of Canada, by the University of Alberta, and by Firmenich SA.

OM980113F

(29) Parker, D. *Chem. Rev.* **1991**, *91*, 1441−1457.

(30) The deuterium-induced isotope effects on ^{1}H nuclear shieldings were typically 8 ppb (*β*-upfield shift) and 10 ppb (α-upfield shift) per deuterium. See: Hansen, P. E. In *Annual Reports on NMR Spectroscopy*; Webb, G. A., Ed.; Academic Press: London, 1983; Vol. 15, pp 105−234.